Available online at www.sciencedirect.com
ScienceDirect
Journal of Power Sources 166 (2007) 303–309
JOURNAL OF POWER SOURCES
www.elsevier.com/locate/jpowsour

Study on water transport in PEM of a direct methanol fuel cell

M.H. Shi *, J. Wang, Y.P. Chen

Department of Power Engineering, Southeast University, Nanjing 210096, PR China

Received 20 May 2005; received in revised form 30 November 2006; accepted 11 December 2006
Available online 24 January 2007

Abstract

Water transport phenomenon in PEM and the mechanism of occurrence and development of a two-phase countercurrent flow with corresponding transport phenomenon in the PEM are analyzed. A one-dimensional steady state model of heat and mass transfer in porous media system with internal volumetric ohmic heating is developed and simulated numerically. The results show that two dimensionless parameters D and N, which reflect the liquid water flow rate and inner heat source in the PEM, respectively, are the most important factors for the water fraction and thermal balance in the PEM. The saturation profiles within the two-phase region at various operating modes are obtained. Smaller mass flow rate of liquid water and high current density are the major contributions to the membrane dehydration.

Keywords: Direct methanol fuel cell; Porous media; Water transport; Dry-out; Two-phase flow

1. Introduction

The direct methanol fuel cell (DMFC), which allows direct use of an aqueous methanol solution as the fuel and air (O_2) as the oxidant, is a new kind of proton exchange membrane fuel cell (PEMFC). Due to its much simpler peripheral units than those of traditional hydrogen PEMFC, which is difficult to safely feed the hydrogen in reality utilization, it has been attached more and more attention [1]. Based on the experimental tests of a DMFC, water and thermal management is one of the key factors, which ensure its highly efficient steady operation and extend its life-span. There has already been quite a few investigations on water and thermal management for a DMFC [2–11], and the prevention of dehydration phenomena in PEM has also been investigated. However, to our knowledge, there is few published literature on the mechanisms of dry-out and burnout phenomena in PEM, which take place in the case of a certain high current density. Usually, water in a working DMFC comes from the aqueous methanol solution fed into the anode, humidified air (O_2) fed into the cathode and the product of cathode electrochemical reaction. With the more abundant sources of water supply, in the most normal operation conditions a DMFC can work under the higher current density without the threat of dehydration of PEM, but in some formidable conditions the burnout of PEM was observed in the tests. Hence, to prevent dry-out and burnout of PEM under high current density will do great help for enhancing the performance and longevity of a DMFC. When current density increases to a certain high value, evaporation and condensation processes of water may go synchronously with its transport in a DMFC. Consequently, to find out the mechanisms of heat and mass transfer in a DMFC is the hard core of water and thermal management. Springer et al. [12] and Springer and Wilson [13] discussed the phenomenon of two-phase transport in traditional hydrogen PEM fuel cells. However, there is still a lack of understanding on the mechanism of occurrence and development of a two-phase flow in a DMFC. In recent years, Wang [14] and his group applied the theory of multiphase, multi-component transport in capillary porous media into the modeling of the PEMFC, and numerically simulated the two-phase flow in porous electrodes considering the evaporation and condensation of water. Then some abnormal phenomena with the concomitant phase change of water, such as cathode flooding, dehydration and dry-out of PEM, etc., which appear in some formidable operation modes, started to be investigated. Since the PEM is very thin and there is only a small range of operating conditions between drying out and flooding of the cathode [11], it is so hard to carry out the visualized experiment of water transportation inside PEM. Thus, to

* Corresponding author. Tel.: +86 25 83792379; fax: +86 25 57712719.
E-mail address: mhshi@seu.edu.cn (M.H. Shi).

0378-7753/$ – see front matter © 2007 Elsevier B.V. All rights reserved.
doi:10.1016/j.jpowsour.2006.12.036

Nomenclature

C	concentration of a species
F	Faraday's constant
h_{fg}	latent heat of evaporation
I	current density
m	mass flux
p	pressure
q	Joule heat flux
S	saturation
T	temperature
$u_{l,d}$	permeability velocity
$u_{l,e}$	electro-osmotic velocity
x	abscissa
Z	charge number of a species

Greek symbols

β	kinematic viscosity ratio
δ	non-dimensional length
ε	porosity
θ	non-dimensional temperature; contact angle
κ	permeability
μ	dynamic viscosity
ν	kinematic viscosity
ρ	density
σ	vapor–liquid interfacial tension
ϕ	electric potential

Subscripts

ac	interface between anode and catalyst layer
l	liquid
s	saturation
v	vapor

understand the transport process of water in PEM, it is essential to develop a theoretical model to analyze the characteristics of water transport in PEM, and explore the mechanism of dry-out of PEM. In this paper, a one-dimensional steady state model of heat and mass transfer in porous media system with internal volumetric ohmic heating is developed and simulated and the mechanisms of occurrence and development of two-phase zone in PEM of a DMFC as a porous media are explored.

2. The flow and phase change in PEM

The standard membrane material used in PEM is a fully fluorinated Telfon-base material. Water transport in hydrophilic membrane is molecular diffusion. Water molecules exist in the pore space of membrane structure. Thus, the water molecular transport in hydrophilic membrane can be considered as a diffusion and permeable process in a porous media with nanometer scale. Therefore, the PEM can be regarded as a porous media system. To analyze the mechanism of water transport in PEM, the PEM porous structure can be simplified as a tube bundle made of solid matrix and void channels, as shown in Fig. 1. PEM is heated from its cathode boundary by heat generated in cathode electrochemical reaction, while ohmic heating contributes to its internal heat source. Under the normal operating conditions, void channels of porous PEM are filled with liquid water and liquid water in the void channel C will be dragged along the channel wall toward cathode side by capillary force. Owing to the current density distribution in cross-section of PEM is usually non-uniform [15], therefore, when the local current density in a certain zone becomes excessively high, the Joule heat produced will be high enough to activate the nucleation of water and then a bubble zone B will occur as shown in Fig. 1a. The water transport in channel makes this evaporation process of water to be continued. Under the function of local Joule heating, the bubbles in the channel will gradually grow up. The whole process seems to be that vapor bubbles move in the opposite direction with liquid water flow in C, while the liquid water in front of the bubble is dragged towards cathode side along the channel wall, and thus form a two-phase countercurrent flow in porous PEM [16]. At the same time, the reduction of liquid water may cause the decrease of local electrical conductivity, which improves the local Joule heating. The higher Joule heating can increase the superheat of water in the cathode side of void channels C and cause a new vapor flow. Thus, the two-phase coexistent zone in porous PEM will appear. Meanwhile, vapor flow is continuously cooled by contact with liquid water in its front and condenses gradually at the interface of liquid–vapor. For a given current density, vapor flow will stop at a certain place of PEM due to the equilibrium between evaporation and condensation. Thus, a local transient two-phase dehydration zone is appeared in PEM, as shown in Fig. 1(b).

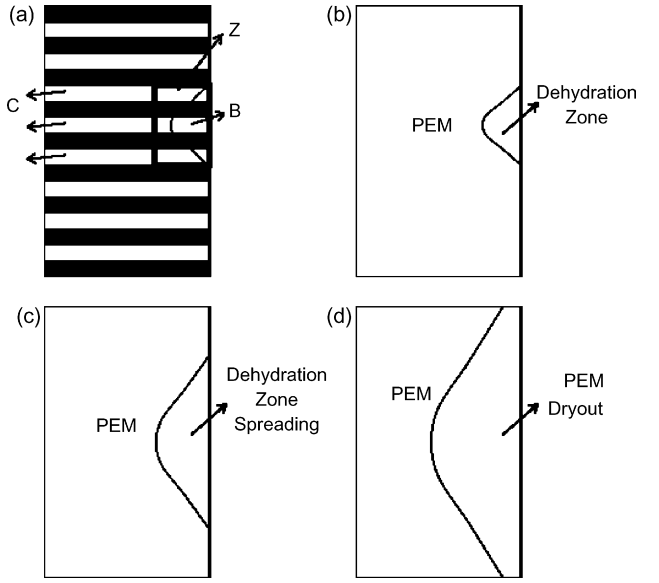

Fig. 1. Evolution of two-phase zone and dryout in PEM (a) Nucleation of water bubble, (b) The formation of a two-phase zone, (c) Spreading of two-phase zone and (d) Dry-out of PEM.

With the increase of the local current density, more vapor bubbles generate and the dehydration zone will spread unboundedly in PEM. On the other hand, the flux of the liquid water dragged by electro-osmotic force increases with the increase of local current density, which may enhance the cooling effect on vapor flow.

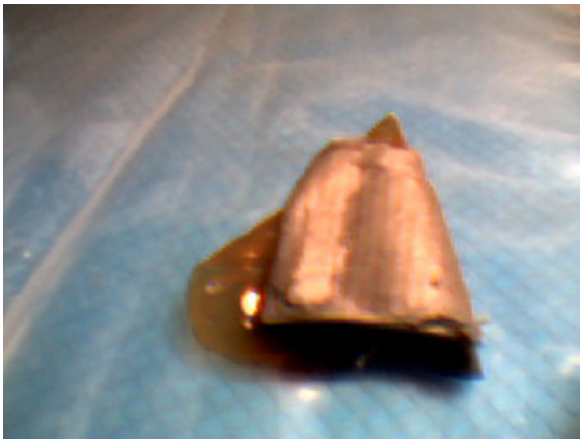

Fig. 2. A burnout sample of PEM.

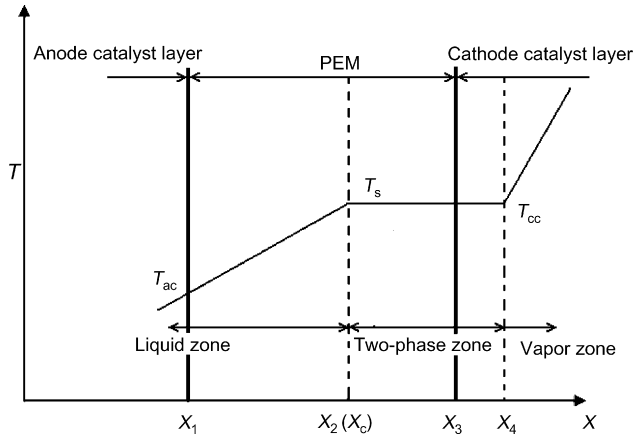

Fig. 3. Temperature distribution in PEM.

Consequently, the development of local two-phase zone with the increase of the current density depends on these two opposite effects as Joule heating and electro-osmotic drag, respectively. The local dehydration zone may spread with the increasing current density, as shown in Fig. 1(c). Under the most of working modes at high current density the normal operation of DMFC can still be conducted. The dehydration zone will not cover the whole cross-section of the interface between PEM and cathode catalyst layer until the local current density reaches to a certain high value. At this moment, most of the void channels in PEM are filled with vapor and PEM is seriously dehydrated owing to liquid water flow collapsing in its cathode side. It causes a large contact resistance and leads to a quick increase of local Joule heat flux. Finally, the temperature of the solid matrix quickly increases, which is the so-called dry-out of PEM, as shown in Fig. 1(d). The dry-out of PEM not only disconnects the internal circuit of a DMFC and causes burnout of PEM as shown in Fig. 2.

3. Analytical model and simulation

The cathode catalyst layer, PEM and anode catalyst layer combine a porous media system. According to the working condition of a DMFC, the system is subjected to a temperature difference such that the temperature at the cathode catalyst layer is significantly higher than the saturation temperature of the interstitial fluid while the anode catalyst layer is maintained below the saturation temperature T_s as shown in Fig. 3.

In this porous media system under the boundary and internal heating, it has been shown that three distinct regions will appear; that is, vapor zone, two-phase zone and liquid zone [17–19]. The thickness of PEM is $l = X_3 - X_1$ and X_c denotes the start point of two-phase zone.

3.1. Water fraction distribution in PEM

To simplify the analysis some assumptions are made as follows:

(1) The local thermodynamically equilibrium in porous PEM is maintained.
(2) Catalyst layers are very thin; they can be treated as the boundaries of PEM.
(3) The flow rate of fluid in porous PEM is low, the inertia force could be neglected and the effect of gravity is also neglected.
(4) The transport properties of liquid and vapor are constant. Liquid water is incompressible and vapor is regarded as ideal gas.

The water velocity from anode to cathode at the liquid zone in PEM can be calculated by Schlögl equation as:

$$u_l = \frac{k_\phi}{\mu_l} Z_f C_f F \frac{\mathrm{d}\phi}{\mathrm{d}x} - \frac{k_p}{\mu_l} \frac{\mathrm{d}p_l}{\mathrm{d}x} = u_{l,e} + u_{l,d} \tag{1}$$

where the first term of right side is the velocity caused by electro-osmotic force and the second is Darcy velocity under a pressure gradient. F is Faraday constant, C_f is the iron density, Z_f is the charge number of iron for a species, ϕ is the electric potential, and k_ϕ, k_p are the electro-osmotic coefficient and permeability of the water in PEM, respectively.

The total water velocity in PEM can be expressed as

$$u_l = u_{l,d} + u_{l,e} \tag{2}$$

The mass flow rate of the liquid water can be calculated as

$$m_l = \rho_l u_l \tag{3}$$

The continuous equation is

$$\frac{\mathrm{d}(\rho_l u_l)}{\mathrm{d}x} = 0 \tag{4}$$

The energy equation under the local thermodynamically equilibrium is:

$$\rho_l C_{pl} u_l \frac{\mathrm{d}T}{\mathrm{d}x} = \frac{\mathrm{d}}{\mathrm{d}x}\left(k_{eff} \frac{\mathrm{d}T}{\mathrm{d}x}\right) + q \tag{5}$$

where C_{pl} is the specific heat capacitance of water, k_{eff} is the effective thermal conductivity of PEM and q is inner volumetric

heat flux produced by Joule heating,

$$q = i\frac{\mathrm{d}\phi}{\mathrm{d}x} \tag{6}$$

The relationship between the current density and the electrical potential as well as electrical conductivity is

$$i = -\sigma_m \frac{\mathrm{d}\phi}{\mathrm{d}x} + FC_f u_\mathrm{l} \tag{7}$$

in which the electrical conductivity σ_m can be expressed as

$$\sigma_m = F^2 D_f + \frac{C_f}{RT} \tag{8}$$

The current continuous equation is

$$\frac{\mathrm{d}\phi}{\mathrm{d}x} = 0 \tag{9}$$

Liquid water in PEM is mainly existed by the form of Hydrate proton (H_3^+O), the diffusion of water in PEM can be neglected. Thus, the mass flow rate of liquid water can be calculated by $\rho_\mathrm{l} u_\mathrm{l}$. Assuming x_c is the coordinate of the interface between liquid zone and two-phase zone. Define the water fraction α_l^x at the location x in PEM as:

$$\alpha_\mathrm{l}^x = \frac{m_\mathrm{l}^x}{m} \tag{10}$$

where m is total mass flow rate of water and m_l^x is liquid flow rate at the location x in PEM.

The average velocity caused by electro-osmotic force and average Darcy velocity in PEM are

$$\bar{u}_\mathrm{l,e} = \frac{k_\phi}{\mu_\mathrm{l}} Z_f C_f F \frac{\Delta\phi}{l} \tag{11}$$

$$\bar{u}_\mathrm{l,d} = \frac{k_p}{\mu_l} \frac{p_\mathrm{ac} - p_\mathrm{s}}{l} \tag{12}$$

where p_s is the pressure at x_c. Thus, the total average liquid water velocity in PEM is

$$\bar{u}_\mathrm{l} = \bar{u}_\mathrm{l,d} + \bar{u}_\mathrm{l,e} \tag{13}$$

The following non-dimensional parameters are defined as

Non-dimensional length $L = \dfrac{x}{l}$

Non-dimensional velocity $U = \dfrac{u_\mathrm{l} - u_\mathrm{l,e}}{\bar{u}_\mathrm{l} - \bar{u}_\mathrm{l,e}}$

Non-dimensional flow rate $M = \dfrac{m}{\rho_\mathrm{l}\bar{u}_\mathrm{l}}$

Non-dimensional temperature $\theta = \dfrac{T - T_\mathrm{s}}{T_\mathrm{ac} - T_\mathrm{s}}$

Non-dimensional pressure $P = \dfrac{p - p_\mathrm{s}}{p_\mathrm{ac} - p_\mathrm{s}}$

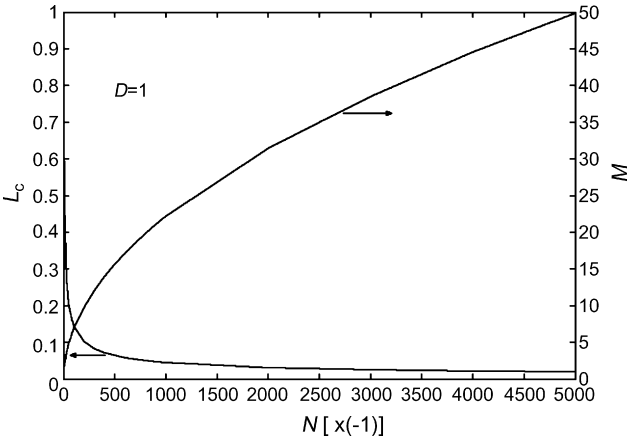

Fig. 4. The start point length of two-phase zone ($D = 1$).

By use of above non-dimensional parameters, Eqs. (4) and (5) become

$$\nabla U = \frac{\mathrm{d}U}{\mathrm{d}L} = 0 \tag{14}$$

$$\frac{\mathrm{d}^2\theta}{\mathrm{d}L^2} - D\frac{\mathrm{d}\theta}{\mathrm{d}L} + N = 0 \tag{15}$$

where $D = C_\mathrm{pl} ml/K_\mathrm{eff}$ and $N = ql^2/(T_\mathrm{ac} - T_\mathrm{s})K_\mathrm{eff}$ are two non-dimensional parameters which reflect the change of water mass flow rate and inner heat source in PEM, respectively.

The boundary conditions are

$$\begin{cases} L = 0, & P = 1, \quad \theta = 1 \\ L = L_\mathrm{c}, & P = 0, \quad \theta = 0 \end{cases} \tag{16}$$

In this paragraph, the water transport phenomena are emphasized and the main objects are the mechanism and development of a two-phase countercurrent flow as well as water fraction distribution in PEM. The numerical simulation was conducted [21] and some calculated results are as follows.

The start point of two-phase zone length L_c (corresponding to $l_\mathrm{c} = X_\mathrm{c} - X_1$) and water fraction distribution in PEM are shown in Figs. 4–7. It is shown that the start point appears ear-

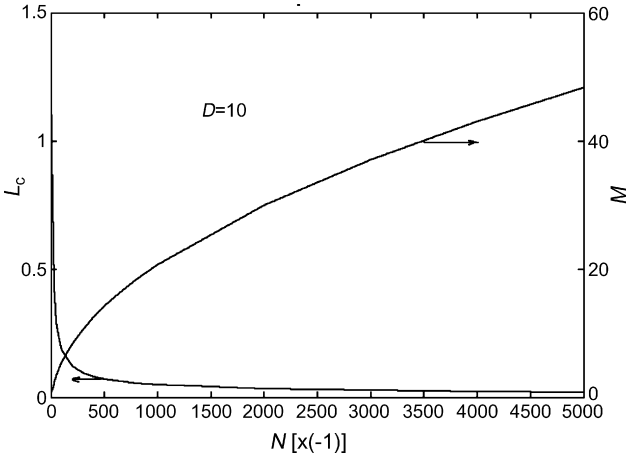

Fig. 5. The start point length of two-phase zone ($D = 10$).

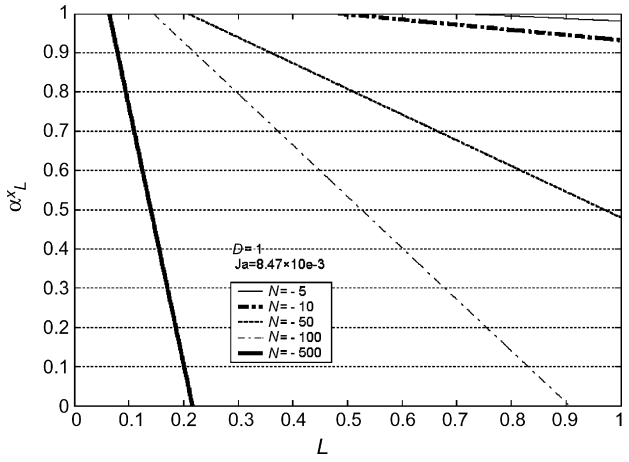

Fig. 6. The water fraction in PEM ($D=1$).

lier at the small water flow rate ($D=1$) when electrical current increases and it causes water fraction in PEM decreasing fast. On the other hand, when the electrical current is small (corresponding to small value of N), the water fraction in PEM is satisfactory to normal operation condition and the dry-out in PEM is never happened. The decrease of the thickness of PEM l will decrease the value of N and it is good for the safe operation.

3.2. The length of two phase zone

The two-phase flow in porous structure of PEM under pressure gradients can be determined by a modified Darcy's equation as

$$u_{\mathrm{l,d}} = -\frac{\kappa\kappa_{\mathrm{rl}}}{\mu_{\mathrm{l}}}\frac{\mathrm{d}p_{\mathrm{l}}}{\mathrm{d}x} \tag{17}$$

$$u_{\mathrm{v}} = -\frac{\kappa\kappa_{\mathrm{rv}}}{\mu_{\mathrm{v}}}\frac{\mathrm{d}p_{\mathrm{v}}}{\mathrm{d}x} \tag{18}$$

The electro-osmotic velocity of liquid water is

$$u_{\mathrm{l,e}} = \frac{\kappa\kappa_{\mathrm{r}\phi}}{\mu_{\mathrm{l}}}Z_f C_f F\frac{\mathrm{d}\phi}{\mathrm{d}x} \tag{19}$$

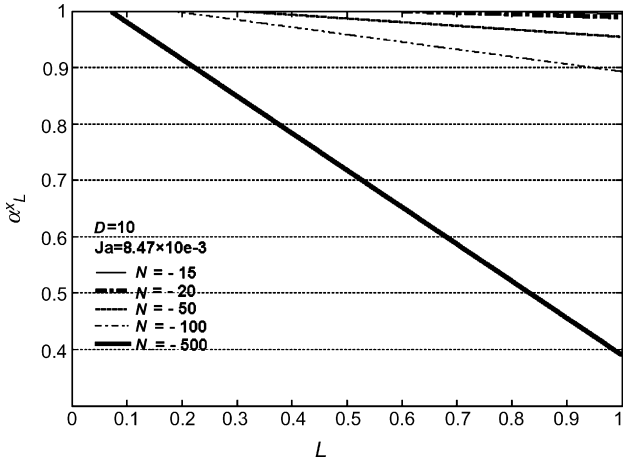

Fig. 7. The water fraction in PEM ($D=10$).

In the above equations, κ_{rl} and κ_{rv} are the relative permeability of the liquid water and vapor, respectively and $\kappa_{\mathrm{r}\varphi}$ is the relative electro-osmotic coefficient of the liquid water.

The mass flow rate of the liquid and vapor phases in two-phase zone are

$$m_{\mathrm{l}} = \rho_{\mathrm{l}}(u_{\mathrm{l,d}} + u_{\mathrm{l,e}}) \tag{20}$$

$$m_{\mathrm{v}} = \rho_{\mathrm{v}} u_{\mathrm{v}} \tag{21}$$

The energy and mass conservation equations in two-phase zone are

$$q = m_{\mathrm{v}} h_{fg} = \frac{i^2 l}{\sigma_m} \tag{22}$$

$$m_{\mathrm{v}} + m_{\mathrm{l}} = 0 \tag{23}$$

Solving Eqs. (17)–(23), the following expressions for vapor pressure, liquid water pressure and capillary pressure gradients are obtained respectively as

$$\frac{\mathrm{d}p_{\mathrm{v}}}{\mathrm{d}x} = -\frac{\nu_{\mathrm{v}} q}{\kappa\kappa_{\mathrm{rv}} h_{fg}} \tag{24}$$

$$\frac{\mathrm{d}p_{\mathrm{l}}}{\mathrm{d}x} = \frac{\nu_{\mathrm{l}} q}{\kappa\kappa_{\mathrm{rl}} h_{fg}} + \frac{\kappa_{\mathrm{r}\phi}}{\kappa_{\mathrm{rl}}} Z_f C_f F\frac{\mathrm{d}\phi}{\mathrm{d}x} \tag{25}$$

$$\frac{\mathrm{d}p_{\mathrm{c}}}{\mathrm{d}x} = -\frac{q}{\kappa h_{fg}}\left(\frac{\nu_{\mathrm{v}}}{\kappa_{\mathrm{rv}}} + \frac{\nu_{\mathrm{l}}}{\kappa_{\mathrm{rl}}}\right) - \frac{\kappa_{\mathrm{r}\phi}}{\kappa_{\mathrm{rl}}} Z_f C_f F\frac{\mathrm{d}\phi}{\mathrm{d}x} \tag{26}$$

To analyze the length of two-phase zone in PEM, the term of water saturation S, which is commonly used in the heat and mass transfer in porous media, is introduced in this paper. In porous PEM the water saturation S is defined as the volumetric percentage of liquid water in a pore volume of PEM with the thickness of $X - X_1$. The relationship between water saturation S and capillary pressure p_{c} in porous media can be correlated by the following expression [22] as

$$f(S) = \frac{p_{\mathrm{c}}}{\sigma\, cos\,\theta_{\mathrm{c}}}\left(\frac{\kappa}{\varepsilon}\right)^{1/2} \tag{27}$$

To simplify the solution, the following non-dimensional parameters are introduced:

Non-dimensional length $\delta = \dfrac{xZ_f C_f F\Delta\phi}{\sigma\ \cos\ \theta_{\mathrm{c}}}\left(\dfrac{\kappa}{\varepsilon}\right)^{1/2}$

Non-dimensional viscosity and permeability $\beta = \dfrac{\upsilon_{\mathrm{l}}}{\upsilon_{\mathrm{v}}}$;

$\gamma = \dfrac{\kappa_{\mathrm{r}\varphi}}{\kappa_{\mathrm{rl}}}$

Non-dimensional pressure $\bar{p}_{\mathrm{v}} = \dfrac{p_{\mathrm{v}} - p_{\mathrm{s}}}{\sigma\ \cos\ \theta_{\mathrm{c}}}\left(\dfrac{\kappa}{\varepsilon}\right)^{1/2}$,

$\bar{p}_{\mathrm{l}} = \dfrac{p_{\mathrm{l}} - p_{\mathrm{s}}}{\sigma\ \cos\ \theta_{\mathrm{c}}}\left(\dfrac{\kappa}{\varepsilon}\right)^{1/2}$

Non-dimensional heat flux $\omega = \dfrac{q\nu_{\mathrm{v}}}{\kappa h_{fg} Z_f C_f F\Delta\phi}$

where σ is surface tension of water and θ_{c} is contact angle.

By use of Eq. (26), Eq. (27) can be rewritten in the following dimensionless form

$$\frac{\mathrm{d}f}{\mathrm{d}\delta} = -\omega\left(\frac{1}{\kappa_{\mathrm{rv}}} + \frac{\beta}{\kappa_{\mathrm{rl}}}\right) - \gamma = f'\frac{\mathrm{d}S}{\mathrm{d}\delta} \tag{28}$$

Solving the Eq. (28), we obtain

$$\frac{\mathrm{d}S}{\mathrm{d}\delta} = \frac{-\omega((1/\kappa_{\mathrm{rv}}) + (\beta/\kappa_{\mathrm{rl}})) - \gamma}{f'} \tag{29}$$

in which κ_{rl}, κ_{rv} and f are selected based on Ref. [20] as

$$f = 1.417(1-S) - 2.120(1-S)^2 + 1.263(1-S)^3 \tag{30}$$

$$\kappa_{\mathrm{rl}} = S^3 \tag{31}$$

$$\kappa_{\mathrm{rv}} = (1-S)^3 \tag{32}$$

Thus, the two-phase zone length can be obtained by integrating Eq. (29) from $X = X_2$, $S = 1$ to $X = X_4$, $S = 0$ as

$$\delta_t = \int_1^0 \frac{f'}{-\omega((1/\kappa_{\mathrm{rv}}) + (\beta/\kappa_{\mathrm{rl}})) - \gamma}\,\mathrm{d}S$$

When the saturation gradient is equal to zero within PEM, the development of two-phase zone goes steadily and saturation will not be changed, thus, there is no vapor zone appearing in the PEM. The dimensionless length of two-phase zone δ_t corresponding to the distance of $|X_4 - X_2|$ can be defined as the theoretical length of two-phase zone, while the actual length of two-phase zone existing in PEM is $|X_3 - X_2|$. Obviously, if the theoretical dimensionless length of two-phase zone $|X_4 - X_2|$ is less than the actual length of two-phase zone $|X_3 - X_2|$, that is, the interface between vapor zone and two phase zone is located inside of PEM, the liquid water flow collapse in its cathode side, the dry-out will exist and the normal operation of cell will be stopped. If the thickness of PEM is far less than the theoretical length of two-phase zone δ_t, the interface between vapor zone and two-phase zone is always located outside of the PEM, the dryout of PEM would not occur at all. These results can explain the existed phenomena reported in literature well, which show that when DMFC works at high current condition, the dry-out is easy to appear and when a DMFC operates in a low current density or the thinner PEM is used, the dry-out and burnout of PEM is hard to occur.

It is found that the parameter $|-\omega/\gamma|$ is a key factor to analyze the characteristics of two-phase zone. A numerical method was proposed to calculate the water saturation S and δ_t [21]. Some calculated results are as follows.

The saturation distribution curves of liquid water in theoretical two-phase zone of PEM under various operating modes are shown in Fig. 8. It shows that at any position where distance $\delta = X - X_2$ is less than $0.54\delta_t$, the saturation increases with the increase of $|-\omega/\gamma|$, while at other position where δ is larger than $0.54\delta_t$, the saturation decreases with the increase of $|-\omega/\gamma|$. Due to $q \propto i^2$, $\Delta\phi \propto i$ and $|-\omega/\gamma| \propto i$, the increase of current density can cause the simultaneous augment of both Joule heat flux and electro-osmotic flux of liquid water. The evaporation of liquid water in two-phase zone by Joule heating may reduce saturation, whereas, the electro-osmotic flux supplies liquid water to two-phase zone of PEM and causes the increase of saturation.

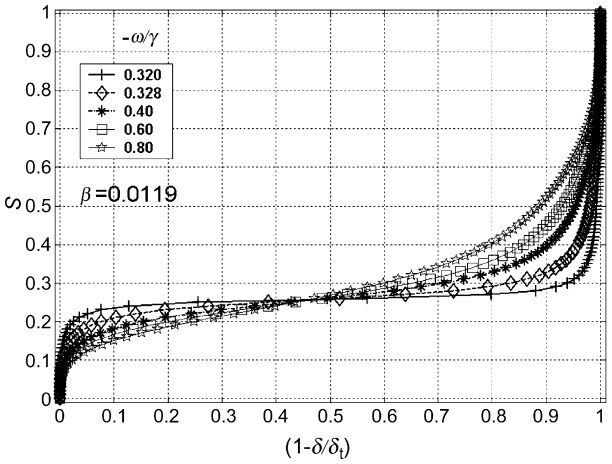

Fig. 8. Liquid saturation profiles with various operating modes.

Within the area where δ is less than $0.54\delta_t$, the higher value of saturation indicates that the local dehydration of PEM is not serious. This means that the increase of current density has a little impact on the augment of Joule heating. When current density increases, the effect of electro-osmotic flux on saturation is strongger than that of Joule heat flux in this area. Conversely, within the area where δ is larger than $0.54\delta_t$, the lower value of saturation indicates that the local dehydration of PEM is very serious, the increase of current density has a large affectation on the augment of Joule heating, so the effect of electro-osmotic flux of liquid water on saturation is weaker than that of Joule heat flux in this area when current density increases. Therefore, creating appropriate boundary conditions in anode and cathode electrodes to maintain a proper length of two-phase zone in PEM has a positive effect on improving performance of a DMFC, which is also an effective way to solve some water management problems, such as cathode flooding and dehydration of PEM. In addition, the evaporation of liquid water in two-phase zone is helpful to prevent burnout of PEM in high temperature by drawing out the Joule heat.

3.3. Pressure distribution in two-phase zone of PEM

The liquid and vapor pressure profiles in two-phase zone of PEM with various operating modes are shown in Fig. 9. For all cases, it is evident that the largest vapor and liquid pressure gradients occur near the liquid zone and vapor zone boundaries, respectively. This is due to the low relative permeability near the endpoints. It is also noted that the middle parts of liquid and vapor pressure profiles approach gradually to be horizontal with the increase of $|-\omega/\gamma|$ (i.e., current density).

Under the low current density conditions, electro-osmotic drag contributes a little to supply liquid water into two-phase zone, while the capillary force dominates the process. Owing to the small average saturation in low current density, the partial pressure gradient of vapor in two-phase zone of PEM is high. In the case of high current density, electro-osmotic drag contributes a lot to the process and counteracts a part of liquid pressure gradient.

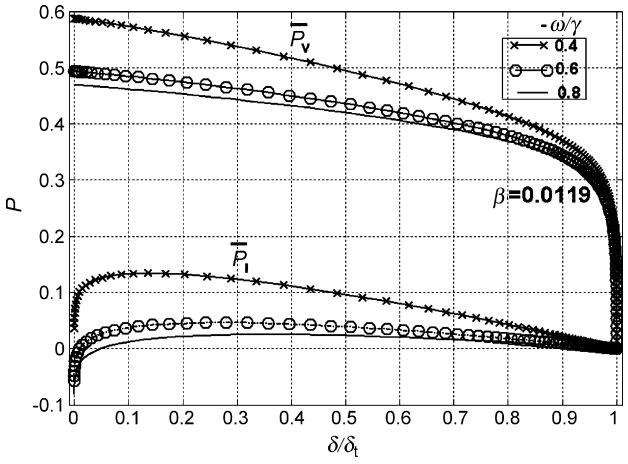

Fig. 9. Liquid and vapor pressure profiles with various operating modes.

4. Conclusions

A one-dimensional porous model for water transport in PEM is developed in this work to analyze water transport characteristics in the PEM. Some major results are obtained and summarized below:

(1) A two-phase zone and vapor–liquid countercurrent flow exist in water saturated porous PEM under some operating conditions. The flow and heat transfer may prevent burnout of PEM under high current density condition.
(2) The start point of two-phase zone and water fraction distribution in PEM are analyzed and calculated. The start point appears earlier at the small water flow rate and it causes water fraction in PEM decreasing fast. When the electrical current is small the water fraction in PEM is satisfactory to normal operation condition and the dry-out in PEM is never happened.
(3) The theoretical length of two-phase zone of PEM is an important non-dimensional parameter to perform the water and heat management of DMFC.
(4) The saturation profiles within the two-phase region at various operating modes are obtained numerically. The results can help to analyze and optimize the performance of a DMFC operating in its ohmic polarization region.

Acknowledgements

The present work is supported by the National Key Basic Research Program of China (no. G2000026303) and the Key Laboratory Foundation of Beijing (KP0504200396).

References

[1] J.H. Hirschenhofer, Fuel Cell Handbook, 6th ed., U.S. Parsons Corporation Reading, 2002.
[2] K. Sundmacher, K. Scott, Chem. Eng. Sci. 54 (1999) 2927–2936.
[3] P. Argyropoulos, K. Scott, J. Power Sources 79 (1999) 169–183.
[4] P. Argyropoulos, K. Scott, J. Power Sources 79 (1999) 184–198.
[5] K. Scott, P. Argyropoulos, J. Electroanal. Chem. 477 (1999) 97–110.
[6] P. Argyropoulos, K. Scott, J. Power Sources 123 (2003) 190–199.
[7] H. Dohle, J. Mergel, J. Power Sources 111 (2002) 268–282.
[8] S. Andrian, J. Meusinger, J. Power Sources 91 (2000) 193–201.
[9] T. Bewer, T. Beckmann, J. Power Sources 125 (2004) 1–9.
[10] M. Craig, Gates, AIChE J. 46 (10) (2000).
[11] A. Siebke, W. Schnurnberger, Fuel cells 3 (1/2) (2003) 37–47.
[12] T.E. Springer, T.A. Zawodzinski, S. Gottesfeld, J. Electrochem. Soc. 138 (1991) 2334.
[13] T.E. Springer, M.S. Wilson, J. Electrochem. Soc. 140 (1993) 3513.
[14] C.Y. Wang, Handbook of Fuel Cells-C Fundamentals, Technology and Applications, vol. 3, Part 3, pp. 337–347. ISBN: 0-471-49926-9.
[15] L. Wang, A. Husar, Int. J. Hydrogen Energy 28 (2003) 1263–1272.
[16] J. Wang, M.H. Shi, Sci. Chin.-E. Technol. Sci. 49 (1) (2006) 102–114.
[17] D.W. Lyons, J.D. Hatcher, Int. J. Heat Mass Transfer 15 (1972) 897–905.
[18] Q. Liao, T.S. Zhao, Int. J. Heat Mass Transfer 43 (2000) 1089–1102.
[19] D. Moalem, Int. J. Heat Mass Transfer 19 (1976) 529–537.
[20] K.S. Udell, Int. J. Heat Mass Transfer 28 (2) (1985) 485–495.
[21] J. Wang, Doctoral Thesis, Southeast University, 2005.
[22] Z.H. Wang, C.Y. Wang, J. Power Sources 94 (2001) 40–50.